J|A|C|S
ARTICLES
Published on Web 04/06/2002

Electron-Rich Three-Center Bonding: Role of s,p Interactions across the p-Block

Markéta L. Munzarová† and Roald Hoffmann*

Contribution from the Department of Chemistry and Chemical Biology, Cornell University, Ithaca, New York, 14853-1301

Received April 9, 2001. Revised Manuscript Received December 5, 2001

Abstract: This paper analyzes the importance of s,p mixing—a necessary addition to the simplest Rundle–Pimentel picture—and periodic and group trends in electron-rich three-center bonding. Our analysis proceeds through a detailed quantum chemical study of the stability of electron-rich three-center bonding in triatomic 22-valence electron anions. To provide interpretations, a perturbational molecular orbital (MO) analysis of s,p mixing is carried out. This analysis of the orbitals and the overlap populations is then tested by density functional calculations for a number of linear trihalides, trichalcogenides, and tripnictides. The most important effect of s,p mixing on the in-line bonding is in destabilization of the $3\sigma_g$ orbital and is determined by the overlap between the s orbital of the central atom and the p orbital of the terminal atom. Further destabilization arises from the repulsion of p_π lone pairs. Both of these antibonding effects increase with increasing negative charge of the system. The stability of isoelectronic X_3 systems thus decreases when moving from right to left in the periodic table. Interesting group trends are discerned; for instance, for the electron-rich tripnictides, the ability to accommodate a hypervalent electron count is the largest in the middle rather at the end of the group. Particularly strong s,p mixing can reverse the bonding/antibonding character of MOs: thus MO $2\sigma_u$ that is responsible for bonding for trihalides and trichalcogenides is actually antibonding in N_3^{7-}.

1. Introduction

The idea of electron-rich three-center bonding in hypervalent molecules, proposed independently by Pimentel[1] and Rundle,[2] celebrates this year its 50th anniversary. Since these seminal contributions, many theoretical studies of the nature of the bonding in hypervalent molecules have been carried out. The concept has been probed in detail, extended, and limited.[3−8] Still, Rundle and Pimentel's scheme remains the basis of the generally accepted view of hypervalency. It invokes a delocalized three-center σ-bonding scheme as shown in structure **1**: three p orbitals combine to give one bonding, one nonbonding, and one antibonding molecular orbital (MO); the lower-lying two orbitals are occupied.

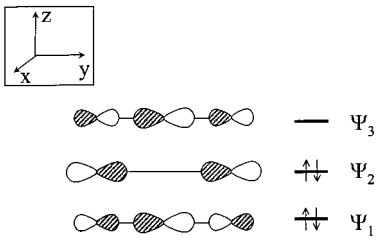

1

This picture captures the essence of electron-rich three-center bonding. But it is oversimplified, most importantly in neglecting a variable amount of s mixing at the central atom in the nonbonding orbital. This s,p mixing in turn is intimately related to the tendency of three-center systems to localize into a bond and a lone pair. A corresponding phenomenon, a Peierls or pairing distortion, occurs with some frequency in extended multicenter systems. Our interest, in this as well as in other papers,[9−11] is to obtain a qualitative understanding of periodic trends in three-center and multicenter electron-rich systems.

As a simple, yet realistic model system we have chosen a series of 22-electron homonuclear triatomic anions. A number of such systems has been observed experimentally. The most abundant group represent trihalides: I_3^-, Br_3^-, and Cl_3^- have been observed in the solid state[6,12−14] and in solution,[12,15] as well as in the gas phase.[16] The F_3^- anion has been observed in

† Current address: National Center for Biomolecular Research, Kotlarska 2, CZ-611 37 Brno, Czech Republic.

(1) Pimentel, C. G. *J. Chem. Phys.* **1951**, *19*, 446.
(2) Hach, R. J.; Rundle, R. E. *J. Am. Chem. Soc.* **1951**, *73*, 4321.
(3) Kutzelnigg, W. *Angew. Chem., Int. Ed. Engl.* **1984**, *23*, 272.
(4) Novoa, J. J.; Mota, F.; Alvarez, S. *J. Phys. Chem.* **1988**, *92*, 6561.
(5) Danovich, D.; Hrušák, J.; Shaik, S. *Chem. Phys. Lett.* **1995**, *233*, 249.
(6) Robertson, K. N.; Bakshi, P. K.; Cameron, T. S.; Knop, O. *Z. Anorg. Allg. Chem.* **1997**, *623*, 104.
(7) Landrum, G. A.; Goldberg, N.; Hoffmann, R. *J. Chem. Soc., Dalton Trans.* **1997**, 3605.
(8) Ogawa, Y.; Takahashi, O.; Kikuchi, O. *J. Mol. Struct. (THEOCHEM)* **1998**, *424*, 285.
(9) Papoian, G. A.; Hoffmann, R. *Angew. Chem., Int. Ed.* **2000**, *39*, 2408.
(10) Seo, D.-K.; Hoffmann, R. *J. Solid State Chem.* **1999**, *147*, 26.
(11) Ienco, A.; Hoffmann, R.; Papoian, G. *J. Am. Chem. Soc.* **2001**, *123*, 2317.
(12) Downs, A. J.; Adams, C. J. In *Comprehensive Inorganic Chemistry*; Bailar, J. C., Jr., Ed.; Pergamon Press: Oxford, U.K., 1973; Vol. 2, p 1534.
(13) Robertson, K. N.; Cameron, T. S.; Knop, O. *Can. J. Chem.* **1996**, *74*, 1572.
(14) Bogaard, M. P.; Peterson, J.; Rae, A. D. *Acta Crystallogr., Sect. B* **1981**, *37*, 1357.
(15) Nelson, I. V.; Iwamoto, R. T. *J. Electroanal. Chem.* **1964**, *7*, 218.
(16) Nizzi, K. E.; Pommerening, C. A.; Sunderling, L. S. *J. Phys. Chem. A* **1998**, *102*, 7674 and references given therein.

rare-gas matrixes[17] and in the gas phase.[18] The trihalide anions have linear and symmetrical structures in solution or in a noble gas matrix.[17] In the solid state they adopt a range of structures from linear to highly asymmetrical structures.[14,19] Triatomic hypervalent anions have further been observed in the solid state for all group 15 elements except nitrogen, in binary and ternary Zintl phases; see ref 20 for Bi_3^{7-}, refs 21and 22 for Sb_3^{7-}, and ref 23 for As_3^{7-}. These high formal charges are screened by counterions in the solid state. In all of these cases, linear symmetrical structures have been observed. The hypervalent P_3^{7-} anion has been reported to have a linear but asymmetrical structure.[24] Two triatomic hypervalent anions have been observed in the chalcogenide group: A linear Te_3^{4-} fragment has been found as a part of a Z-shaped Te_5^{4-} anion in NaTe,[25] and a linear Se_3^{4-} fragment has been reported (in both symmetrical and asymmetrical forms) in a ternary niobium selenide.[26]

Besides these systems, we include in our study two hypothetical linear anions. The first is N_3^{7-}, a system related to the imagined linear N^{2-} chain studied in ref 9. This system is a pedagogically useful example of maximal s,p mixing. The second is a Sn_3^{10-} anion considered in ref 11. This linear Sn_3 anion is a hypothetical building block of 2D slabs of Sn atoms found in the unusual LiSn phase. The actual electron count in this structure is lower than that expected from the usually reliable extended Zintl−Klemm concept (see ref 9 and references given therein). One of our aims in this work was to understand the factors that so strongly disfavor the formation of electron-rich N_3^{7-} and Sn_3^{10-} but do not prevent the formation of many other isoelectronic electron-rich anions.

We begin our study with qualitative considerations of the orbital interactions in electron-rich three-center bonded systems, based on the one-electron philosophy of the Hückel molecular orbital (HMO) method, with overlap included. With the help of the perturbational molecular orbital (PMO) method,[27] we are led to focus on the factors influencing the four-electron repulsions between the doubly occupied orbitals. The conclusions emerging from the PMO analysis are then tested by density-functional calculations on the 12 isoelectronic anions discussed above. In particular, overlap populations and orbital interaction energies are analyzed in terms of orbital contributions, followed by an interpretation of the observed trends. Finally, a number of general conclusions and a simplified bonding model are provided.

2. Computational Methodology

All calculations have been performed on 22-valence electron X_3 species possessing idealized $D_{\infty h}$ symmetry. For I_3^-, we used the bond length of 2.93 Å, determined from two regressions (25 and 21 samples, respectively) of bond lengths for discrete I_3^- anions in crystals.[12] Similarly, the bond length used for Br_3^- has been determined from two regressions (32 asymmetric Br_3^- anions and 14 Br_3^- symmetric anions) of bond lengths in crystals.[6] For Cl_3^-, we are aware of only one X-ray structure determination, reporting an almost linear and asymmetric structure [2.227(4), 2.305(3) Å].[14] Our calculations have been performed on a symmetric structure with bond lengths given by the geometric average (2.27 Å) of observed bond lengths. To the best of our knowledge, there exist no experimental data on the F−F bond lengths in F_3^-; we have thus adopted the density functional theory (BP86) optimized structure of 1.77 Å.[7] For the Te_3^{4-} anion, the experimental Te−Te bond length of 3.08 Å has been used. For Se_3^{4-} we used the bond length in the symmetrical anion, 2.64 Å (a slightly asymmetrical anion with bond lengths of 2.59 and 2.63 Å has also been observed in the same structure).[26] For Bi_3^{7-}, we use the bond length of 3.43 Å obtained in $Sr_{14}MnBi_{11}$; the other two X-ray structures reported in the same work gave Bi−Bi distances of 3.34 Å ($Ca_{14}MnBi_{11}$) and 3.50 Å ($Ba_{14}MnBi_{11}$). We are aware of two experimental structures for Sb_3^{7-};[21,22] of these we have chosen the Sb−Sb bond length of 3.26 Å obtained for $Eu_{14}MnSb_{11}$ by Rehr and Kauzlarich.[22] The As−As bond length used for As_3^{7-} was 2.96 Å, from the only available X-ray structural data.[23] For P_3^{7-}, our calculations have been performed for a bond length given by the geometric average (2.90 Å) of the two experimental bond lengths in the asymmetric anion (2.52 and 3.34 Å).[24,28]

For N_3^{7-}, there is no experimental structure available, and a geometry optimization is difficult to perform due to the high negative charge of the anion. We were thus forced to make an arbitrary choice; we decided to use an N−N distance of 1.75 Å. This was motivated by the fact that the bond lengths in electron-rich trihalides are usually 0.3 Å longer than the bond lengths in corresponding normal diatomic halogens.[7] We supposed that a similar bond elongation could be expected for N_3^{7-} with respect to a single bond between two nitrogens (1.45 Å). For Sn_3^{10-}, we used the bond length of 3.17 Å, which is an average Sn−Sn distance in the 2D slab of Sn atoms in LiSn.[11]

The formal charges on most of the systems are very high. Indeed, most of these ions exist only in the solid, surrounded by countercations. In the gas phase, we expect all the anions except trihalides to be unbound. How to deal with these large negative charges in the theory? A standard approach to take into account the effect of the crystalline environment is to replace the atoms outside the calculated molecule with point charges.[29] The effects of all point charges are then summed up to convergence by a Madelung-type treatment.[30] The Madelung potential is evaluated on a point grid in the vicinity of the molecular group and is then simulated by fitted charges at a finite number of surrounding points of the real crystal lattice.[29,31−33]

Our aim was to model the electrostatic stabilization in a simpler way, one that would allow us to compare different systems without the need to refer to specific crystal environments. The motivation for doing so was our desire to treat in a consistent way real triatomic units found in crystals, together with hypothetical systems (N_3^{7-}), as well as mono- and diatomic fragment anions. Any model that avoids the explicit treatment of the crystal lattice is, by definition, only a rough approximation of the true Madelung potential experienced by the anion. However, we believe that, if reasonably chosen, such a model still makes possible a meaningful comparison of orbital interactions in a set of isoelectronic systems.

(17) (a) Ault, B. S.; Andrews, L. *J. Am. Chem. Soc.* **1976**, *98*, 1591. (b) Ault, B. S.; Andrews, L. *Inorg. Chem.* **1977**, *16*, 2024. (c) Hunt, R. D.; Thompson, C.; Hassanzadeh, P.; Andrews, L. *Inorg. Chem.* **1994**, *33*, 388.
(18) (a) Tuinman, A. A.; Gakh, A. A.; Hinde, R. J.; Compton, R. N. *J. Am. Chem. Soc.* **1999**, *121*, 8397. (b) Artau, A.; Nizzi, K. E.; Hill, B. T.; Sunderlin, L. S.; Wenthold, P. G. *J. Am. Chem. Soc.* **2000**, *122*, 10667.
(19) In the solid state, packing forces normally cause small deviations from linearity. We will refer to all structures with an angle at the central atom > 165° as linear.
(20) Kuromoto, T. Y.; Kauzlarich, S. M.; Webb, D. J. *Chem. Mater.* **1992**, *4*, 435.
(21) Cordier, G.; Schäfer, H.; Stelter, M. *Z. Anorg. Allg. Chem.* **1984**, *519*, 183.
(22) Rehr, A.; Kauzlarich, S. M. *J. Alloys Comp.* **1994**, *207*, 424.
(23) Kauzlarich, S. M.; Thomas, M. M.; Odink, D. A.; Olstead, M. M. *J. Am. Chem. Soc.* **1991**, *113*, 7205.
(24) Vaughey, J. T.; Corbett, J. D. *Chem. Mater.* **1996**, *8*, 671.
(25) Böttcher, P.; *J. Less-Common Met.* **1985**, *109*, 311. See also ref 26.
(26) Dürichen, P.; Bolte, M.; Bensch, W. *J. Solid State Chem.* **1998**, *140*, 97.
(27) Albright, T. A.; Burdett, J. K.; Whangbo, M.-H. *Orbital Interactions in Chemistry*; Wiley & Sons: New York, 1985.
(28) Even when asymmetric, the anions can be reliably fitted to a hyperbolic d_1/d_2 relationship, which in turn gives an estimate of a symmetrical X−X distance. See Bürgi, H. B., Dunitz, J. D., Eds. *Structural Correlations*; Wiley−VCH: Weinheim, Germany, 1994; Vol. 1, p 2.
(29) Liao, M.-S.; Zhang, Q.-E. *J. Phys. Chem. A* **1998**, *102*, 10647.
(30) Ewald, P. P. *Ann. Phys.* **1921**, *64*, 253.
(31) Liao, M.-S.; Zhang, Q.-E. *J. Solid State Chem.* **1999**, *146*, 239.
(32) Liao, M.-S.; Huang, S.-P. *J. Organomet. Chem.* **2000**, *598*, 374.
(33) Mödl, M.; Dolg, M.; Fulde, P.; Stoll, H. *J. Chem. Phys.* **1997**, *106*, 1836.

Our model simulates the electrostatic stabilization by distributing a set of partial positive charges that in their sum exactly compensates the negative charge of the anion over a surface defined as follows: For the monatomic fragments, the charge was put on the surface of a sphere, whose radius was given by the bonding distance in the corresponding electron-rich trianion. For a diatomic fragment, the surface was defined by a superposition of the two spheres defined above, whereas for triatomic systems three such spheres centered on constituent atoms were used. The point charges were placed only on the "outside" of the composite surface, distributed at points disposed as are the C nuclei in buckminsterfullerene; altogether we used 60, 80, and 120 point charges for mono-, di-, and triatomic anions, respectively. Such a charge distribution stabilized all systems sufficiently, in the sense that the eigenvalues of all occupied Kohn−Sham (KS) orbitals were negative; the only exceptions to this were N_2^{4-} (one positive KS eigenvalue) and N_3^{7-} (two positive KS eigenvalues). Of course, in the absence of these positive ion atmospheres, many of the KS eigenvalues would be positive.

The calculations were carried out with the Amsterdam Density Functional (ADF1999.02) program.[34−37] We employed the BP86 functional, which combines Becke's GGA functional for exchange[38] with Perdew's GGA for correlation.[39] The valence atomic orbitals were represented by a basis set of Slater-type orbitals. Triple-ζ basis sets from the ADF database were used, which include one polarization function for H through Ar and for Ga through Kr. The core atomic orbitals were frozen out to 1s (N, F), 2p (P, Cl), 3p (As, Se, Br), 4p (Sn, Sb, Te, I), and 5p (Bi).

Throughout this work, we make extensive use of the fragment orbital analysis available in ADF. Our approach is based on the formation of the $X_3^{(3k+1)-}$ system from one terminal atom (X_T), with a negative charge of $k + 1$, and the rest of the molecule (X_C-X_T unit, C = central atom, T = terminal atom), with a negative charge of $2k$ and a bond distance as in $X_3^{(3k+1)-}$. Most of our interpretation is based on a Mulliken population analysis (MPA), which for any one-electron approximation is completely defined by (1) assigning the atoms to the fragments and (2) the set of basis functions on each center. Thus, the MPA is independent of the particular charge partitioning.

The specification of fragment charges is, however, necessary for the energy decomposition procedure. Within ADF, bonding energies between fragments of molecule are decomposed by the transition-state (TS) procedure of Ziegler.[40] This scheme breaks interaction energies into several chemically intuitive contributions. Of these, the Pauli (or exchange) repulsion term is directly related to "four-electron two-orbital" interactions in qualitative molecular orbital theory.[40,27] It is determined by the change in density due to mutual orthogonalization of the occupied orbitals on the two fragments. We adopted the charge partitioning between the fragments chosen (X_T bearing one more electron than the X_C-X_T fragment) in order to study the formation (breaking) of a bond between two atoms with different formal charges. This is the situation encountered in electron-rich three-center bonded systems, where negative charge concentrates on the terminal atoms.[27]

3. Qualitative Symmetry and Perturbational Considerations

Within the HMO method, the MOs of a 22-valence electron X_3 system are constructed from valence (s and p) atomic orbitals of each atom. For homonuclear systems, the component

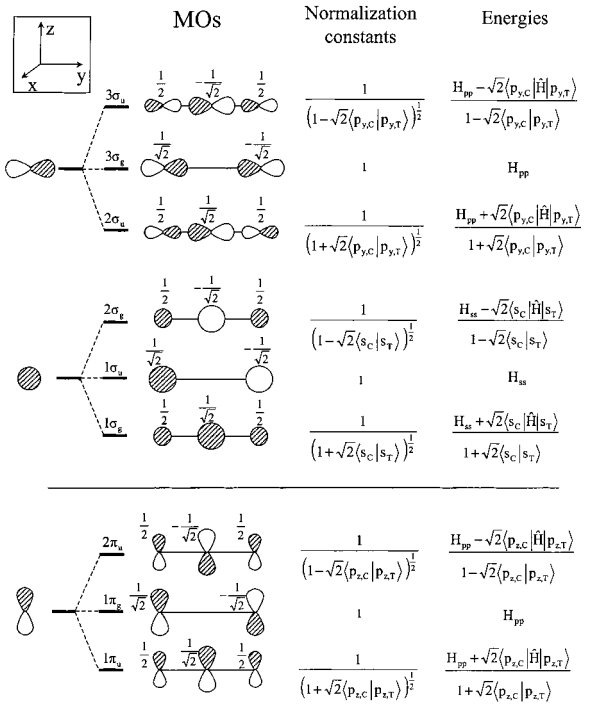

Figure 1. HMO (with overlap included) solutions of the secular equations for the s(σ), p(σ), and p(π) interactions, each considered separately.

interacting levels (s or p) are degenerate for a given angular momentum type (s−s, p−p). For purposes of interpretation, it is useful to separate these degenerate interactions from the nondegenerate (s−p) ones. Therefore, we build MOs of X_3 by first neglecting all s−p overlap matrix elements and solving the secular equations separately for s and p orbitals. Then we include the nondegenerate interactions (s,p mixing) as a perturbation. This approach is common for the construction of MOs of homonuclear diatomic molecules.[27,41,42] It presumes that the degenerate interactions between orbitals of the same type (s or p) result in an energy splitting that is significantly larger than the matrix elements of the perturbation between orbitals of different type (s with p).[43]

The secular equations for the s(σ), p(σ), and p(π) interactions between degenerate levels are all of the same type and can be solved analytically at the Hückel level, with overlap included. For solutions and schematic drawings of MOs, see Figure 1. Only one of the two p(π) interactions is shown. The π (p_x, p_z) orbitals are placed at the bottom of the figure, not because they are there energetically but to prepare for the important mixing, which is between the s and p_y orbitals.

For a 22-valence electron system, all levels except the highest one, $3\sigma_u$, are occupied. The latter orbital is the antibonding combination resulting from the p(σ) interaction; it is only the fact that this MO is empty that holds these systems together. The occupied nonbonding $3\sigma_g$ and bonding $2\sigma_u$ orbitals represent the classical electron-rich three-center bond.[1,2] While $3\sigma_g$ is nonbonding, $2\sigma_u$ contributes positively to the total overlap population and decreases the total energy. Both the contribution

(34) Baerends, E. J.; Ellis, D. E.; Ros, P. *Chem. Phys.* **1973**, *2*, 41.
(35) Versluis, L.; Ziegler, T. *J. Chem. Phys.* **1988**, *88*, 322.
(36) te Velde, G.; Baerends, E. J. *J. Comput. Phys.* **1992**, *99*, 84.
(37) Fonseca Guerra, C.; Snijders, J. G.; te Velde, G.; Baerends, E. J. *Theor. Chem. Acc.* **1998**, *99*, 391.
(38) Becke, A. D. *Phys. Rev. A* **1988**, *38*, 3098.
(39) (a) Perdew, J. P.; Wang, Y. *Phys. Rev. B* **1986**, *33*, 8822. (b) Perdew, J. P.; Wang, Y. *Phys. Rev. B* **1986**, *34*, 7406.
(40) Ziegler, T. In *Metal−ligand interactions: from atoms, to clusters, to surfaces*; Salahub, D. R., Russo, N., Eds.; Kluwer: Dordrecht, The Netherlands, 1992; p 367.
(41) Seo, D.-K.; Papoian, G.; Hoffmann, R. *Int. J. Quantum Chem.* **2000**, *77*, 416.
(42) Jean, Y.; Voltaron, F. *An Introduction to Molecular Orbitals*; Oxford University Press: Oxford, U.K., 1993.
(43) Our EH calculations on the I_3^- system in fact showed that the energy splitting due to the interaction of nondegenerate levels is on the average 25−30% of the splitting due to the interactions of the degenerate levels.

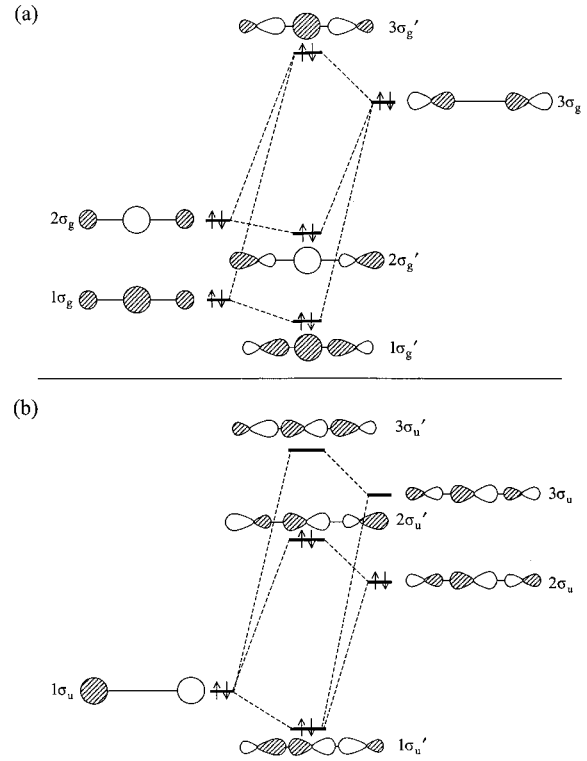

Figure 2. Effect of s,p mixing on the σ orbitals to first-order in PT: a summary of interactions for linear X_3.

to the overlap population and the contribution to energy have an approximate linear dependence on the overlap between the interacting atomic orbitals of the central atom and the terminal atoms.[27]

Lower lying, the s(σ) and the two p(π) interactions are repulsive, as all participating orbitals are fully occupied. These orbital sets decrease the total overlap population and increase the total energy; both of these contributions have a quadratic dependence on the overlap between interacting orbitals of the neighboring atoms.[27] For the trihalides bearing a single negative charge, the magnitudes of the orbital interactions decrease rapidly in the order p(σ) > s(σ) > p(π), following the same trend in the $\langle p_{y,C}|p_{y,T}\rangle$, $\langle s_C|s_T\rangle$, and $\langle p_{x,C}|p_{x,T}\rangle$ ($\langle p_{z,C}|p_{z,T}\rangle$) overlaps. With increasing negative charge of the system, however, the magnitude of the p(π) interaction strongly increases, as we will see below.

In the next step, we turn on s,p interaction and analyze the outcome by means of perturbation theory (PT) with inclusion of overlap.[27,41] The additional orbital mixing is schematically shown in Figure 2, with the interactions partitioned by g and u symmetry type.

$1\sigma_g$ and $2\sigma_g$ will mix into $3\sigma_g$ and destabilize it (Figure 2a). As $1\sigma_g$ and $2\sigma_g$ are orthogonal, there will be no first-order mixing between them.[44] In this sense, $1\sigma_g-3\sigma_g$ and $2\sigma_g-3\sigma_g$ interactions can be treated as mutually independent. Analogously, there will be $1\sigma_u-2\sigma_u$ and $1\sigma_u-3\sigma_u$ interactions, resulting in a stabilization of $1\sigma_u$ and a destabilization of both $2\sigma_u$ and $3\sigma_u$ (Figure 2b), but no first-order $2\sigma_u-3\sigma_u$ mixing. Thus, any of the three-orbital interactions shown in Figure 2 can be viewed as being composed of two two-orbital interactions

(44) There will be, however, second-order mixing between $1\sigma_g$ and $2\sigma_g$ via the $1\sigma_g-3\sigma_g$ and $2\sigma_g-3\sigma_g$ interactions; see refs 27 and 41.

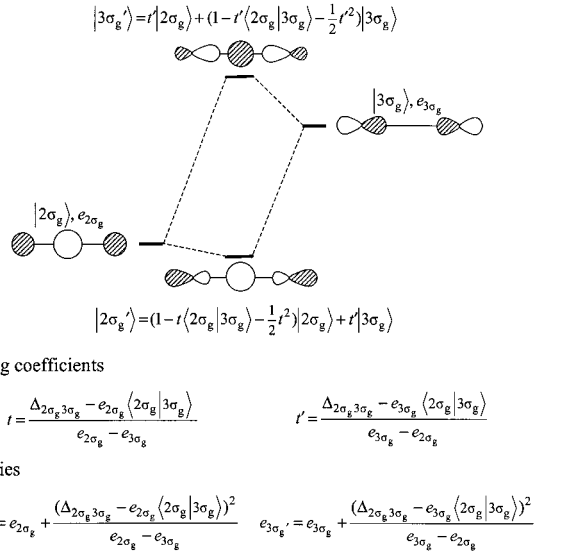

Figure 3. Wave functions and energies for the interaction between $2\sigma_g$ and $3\sigma_g$, the consequence of s,p mixing to first-order in the wave functions.

affecting one orbital. The orbital admixtures to the "shared MO" ($3\sigma_g$ or $1\sigma_u$) will be additive, to first-order in PT. A generic diagram describing these first-order s−p interactions is shown in Figure 3 (orbital icons and PT expressions are given for MOs $2\sigma_g$ and $3\sigma_g$, but the same formulas apply for any pair of MOs).[45]

The main question we want to address in this work is what will be the effect of these mixings on the total orbital interaction energy and the total overlap population in X_3. This, of course, depends on the occupation of the interacting levels. The only interaction involving two electrons is that of $1\sigma_u$ with $3\sigma_u$ (see Figure 2b). It will result in an energy stabilization given by $2(e_{1\sigma_u'} - e_{1\sigma_u})$. This energy stabilization will be proportional to the square of overlap of the interacting orbitals and inversely proportional to their energy difference, as the explicit expressions in Figure 3 indicate. Throughout this paper unprimed orbitals and energies refer to the unperturbed basis functions for the PT treatment, while primed terms are after perturbation.

What redistribution of electron density should be expected due to this interaction? The electron density associated with $1\sigma_u'$ is

$$1 = \langle 1\sigma_u'|1\sigma_u'\rangle = (1 - 2t\langle 1\sigma_u|3\sigma_u\rangle - t^2)\langle 1\sigma_u|1\sigma_u\rangle + 2t\langle 1\sigma_u|3\sigma_u\rangle + t^2\langle 3\sigma_u|3\sigma_u\rangle \quad (1)$$

Thus, an amount of the electron density given by $2t\langle 1\sigma_u|3\sigma_u\rangle$, which was located in the nonbonding orbital $1\sigma_u$ (see Figure 2b), is now shared by $1\sigma_u$ and $3\sigma_u$. The part of this shared density that is associated with the central atom coefficient in $3\sigma_u$ contributes to the bonding. Thus, the contribution of this particular interaction to the bonding between the central atom and the terminal atoms is given by $4ct\langle 1\sigma_u|3\sigma_u\rangle$, where c represents the coefficient of the central atom in $3\sigma_u$. Multiplication by a factor of 2 is due to the participation of two electrons in this orbital interaction. As t is proportional to $\langle 1\sigma_u|3\sigma_u\rangle$ (compare Figure 3 and note that Δ_{ij} is proportional to orbital overlap, according to the Wolfsberg−Helmholtz formula),[27,46]

(45) The first-order wave functions shown in Figure 3 (up to the order of t^2) have been normalized by including the second-order self-interaction terms.

(46) (a) Mulliken, R. S. *J. Chim. Phys.* **1949**, *46*, 497, 675. (b) Wolfsberg, M.; Helmholtz, L. *J. Chem. Phys.* **1952**, *20*, 837.

this positive contribution to the overlap population is proportional to $\langle 1\sigma_u|3\sigma_u\rangle^2$, i.e., to the square of overlap of the interacting orbitals. And as t is indirectly proportional to ($e_{1\sigma_u} - e_{3\sigma_u}$), we do not expect the overall stabilization or bonding due to this interaction to be great, simply because $1\sigma_u$ and $3\sigma_u$ are so far apart in energy. For the same reason, the amount of electron density given by t^2 that was located in the nonbonding orbital $1\sigma_u$ and is now located in the antibonding MO $3\sigma_u$ (see eq 1) will be negligible.

Let us now focus on the more numerous interactions involving four electrons. In these the antibonding combination in Figure 3 will be occupied. For the interaction between $2\sigma_g$ and $3\sigma_g$, the energy stabilization due to $2\sigma_g'$ occupation is overcompensated by the energy destabilization due to $3\sigma_g'$ occupation. The net energy loss is given by

$$\Delta E = -4\langle 2\sigma_g|3\sigma_g\rangle\left(\Delta_{2\sigma_g 3\sigma_g} - \frac{e_{2\sigma_g} + e_{3\sigma_g}}{2}\cdot\langle 2\sigma_g|3\sigma_g\rangle\right) \quad (2)$$

i.e., it is proportional to the square of the overlap of interacting orbitals.

What redistribution of electron density follows for four-electron occupation? The topology of all the first-order mixings we discuss here is the same: An orbital that has zero coefficient on the central atom, and is thus nonbonding, interacts with an orbital with nonzero central atom coefficient. Therefore, for any orbital interaction we can apply what we have derived above for the interaction of $1\sigma_u$ with $3\sigma_u$. There will always be a positive contribution to the OP given by $4ct\langle m\sigma|n\sigma\rangle$, where c represents the coefficient of the central atom in the orbital where it is nonzero.[47] But, due to the occupation by four electrons, there will be also a negative contribution to the OP given by $4ct'\langle m\sigma|n\sigma\rangle$, as t' is negative for a positive $\langle m\sigma|n\sigma\rangle$ overlap (see Figure 3; in the expression for t', the numerator is negative whereas the denominator is positive). The net change in the overlap population will be given by

$$\tilde{P}_{m\sigma n\sigma} = 4ct\langle m\sigma|n\sigma\rangle + 4ct'\langle m\sigma|n\sigma\rangle = 8c\langle m\sigma|n\sigma\rangle^2 \quad (3)$$

So, while each of the first-order mixing coefficients (t and t') is directly proportional to the overlap of the interacting orbitals ($\Delta_{ij} \propto -\langle i|j\rangle$) and inversely proportional to their energy difference, the sum $t + t'$, and thus also the total change in the overlap population, depends on the square of the overlap only.

For interactions between doubly occupied orbitals $m\sigma$ and $n\sigma$, $\langle m\sigma|n\sigma\rangle^2$ is thus the main factor determining the net decrease of overlap population. As will be shown below, this explains the quadratic dependence of OP in Sn_3^{10-} on the Sn−Sn distance reported by Ienco et al.,[11] as well as the strong influence of STO exponents vs negligible influence of H_{ii}s on total OP found in the same work.

4. Summary of Qualitative Considerations of s,p Mixing

Having analyzed the orbital interactions in detail, let us summarize and see what are the net effects of s,p mixing in σ_u and σ_g symmetries on the bonding. In σ_g symmetry, both the $1\sigma_g-3\sigma_g$ and the $2\sigma_g-3\sigma_g$ interactions involve four electrons and their destabilizing effects thus reinforce each other.[27] In σ_u symmetry, the four-electron (4e) destabilizing $1\sigma_u-2\sigma_u$ interaction is compensated by the two-electron (2e) stabilizing $1\sigma_u-3\sigma_u$ interaction. Therefore, we expect the bond-weakening effect of the first-order mixing in σ_g symmetry to dominate over the effect of first-order σ_u mixing. It is much more difficult to predict the relative contributions of the first-order σ_g mixing and the other destabilizing interactions—s(σ) and p(π) zeroth-order mixings—to the total overlap population. This will be discussed in more detail in the next section.

The net effect of the first-order mixing in σ_g symmetry on the total OP is determined by the overlap of the zeroth-order σ_g MOs. $3\sigma_g$ is composed purely of p_y orbitals of terminal atoms and has nonzero overlap only with central atom contributions to $2\sigma_g$, $1\sigma_g$.[48] Two factors influence the overlap between a p_y orbital of X_T and X_C contributions to $2\sigma_g$, $1\sigma_g$: (1) the overlap between s and p orbitals of two atoms (ions) at the particular X_C-X_T distance ($\langle s_C|p_T\rangle$) and (2) the central s-orbital coefficient in $2\sigma_g$, $1\sigma_g$ (given by $\langle s_C|s_T\rangle$; see Figure 1). We expect that the $\langle s_C|p_T\rangle$ term can be considered as the controlling factor. The first reason for this is that within the most simple existing description, the simple Hückel method without overlap, $\langle s_C|p_T\rangle$ is the only factor determining overlap between $3\sigma_g$ and $2\sigma_g$, $1\sigma_g$. Second, we expect the $\langle s_C|p_T\rangle$ and $\langle s_C|s_T\rangle$ overlap integrals to be correlated over the range of interatomic distances encountered in the hypervalent anions. This will be confirmed below by the results of our density functional theory (DFT) calculation.

5. Quantitative Aspects and Periodic Trends

The qualitative considerations outlined above provide a framework for understanding s,p mixing in electron-rich systems. We need, however, a quantitative underpinning of this analysis. To this end we have performed a series of density functional calculations, followed by Mulliken population analysis and an energy decomposition procedure. We recall that our analysis is based on the formation of the X_3 system from one terminal atom and the rest of the molecule. In the following, by "total overlap population" we will always mean the overlap population between the two fragments defined above. The contribution of a particular MO to the total overlap population will be sometimes shortened to "MO overlap population".

As we explained above, $\langle s_C|p_T\rangle^2$ is expected to be one of the important factors influencing the contribution of orbitals of σ_g symmetry to the total OP. To calculate these and other overlap integrals from the qualitative MO considerations at the DFT level, we have performed density functional calculations on two atomic fragments, one representing the central atom X_C and the other the terminal atom X_T. Wishing to model the higher electron density at the terminal atoms of the electron-rich three-center bonded systems,[27] for purposes of calculation we assigned a negative charge of k to an X_C, and a charge $k + 1$ to X_T (when the X_3 molecule bears a $3k + 1$ charge). We then calculated overlaps between corresponding valence atomic orbitals in X_T and X_C at a separation equal to the bond length in X_3.

The results of the fragment population analysis, broken down orbital by orbital in Table 1, provide us with many useful insights. Looking first at the last column, the total OP, we see that the total overlap populations are close to zero for all

(47) Here we drop the u/g symmetry labels, as our discussion in this section applies to orbital interactions of both gerade and ungerade symmetry.

(48) That is, 1,3 interactions are neglected; note that s and p orbitals on the same center are orthogonal.

Table 1. Overlap Population: Orbital Contributions and Sum[a]

molecule	$1\sigma_g$	$2\sigma_g$	$3\sigma_g$	$1\sigma_u$	$2\sigma_u$	$1\pi_u$	$1\pi_g$	$2\pi_u$	total
F_3^-	0.08	−0.12	−0.08	−0.04	0.12	0.16	0.00	−0.16	−0.06
Cl_3^-	0.16	−0.12	−0.20	0.04	0.16	0.24	0.00	−0.40	−0.10
Br_3^-	0.12	−0.12	−0.12	0.04	0.20	0.24	0.00	−0.40	−0.06
I_3^-	0.12	−0.12	−0.24	0.04	0.16	0.24	0.00	−0.40	−0.18
Se_3^{4-}	0.16	−0.16	−0.56	0.04	0.20	0.48	0.00	−0.96	−0.82
Te_3^{4-}	0.16	−0.16	−0.60	0.08	0.20	0.40	0.00	−0.88	−0.86
N_3^{7-}	0.24	−0.08	−1.36	0.24	−0.12	0.64	−0.16	−1.52	−2.12
P_3^{7-}	0.16	−0.08	−0.72	0.12	−0.04	0.56	−0.08	−1.44	−1.52
As_3^{7-}	0.12	−0.08	−0.84	0.12	0.00	0.56	−0.08	−1.44	−1.60
Sb_3^{7-}	0.16	−0.12	−1.04	0.12	0.08	0.56	−0.08	−1.84	−2.12
Bi_3^{7-}	0.16	−0.16	−1.16	0.12	0.08	0.56	−0.08	−1.76	−2.18
Sn_3^{10-}	0.24	−0.24	−2.04	0.20	−0.12	0.80	−0.32	−3.84	−5.28

[a] Overlap population between the X_T and X_C-X_T fragments in X_3. BP86 results.

trihalides and decrease greatly with the charge on the system. With interfragment overlap populations being negative, what binds these systems? In fact, as was noted earlier, the majority of the X_2-X bonding energy arises from electrostatic effects, in the way these are defined in the DFT partitioning scheme.[40] The stabilizing force of the orbital interactions expresses itself more in the control of geometry than in the binding energy.[7] Second, a great part of the negative overlap population comes from the occupation of $3\sigma_g$ and $2\sigma_g$. But repulsive interactions of π symmetry are of equal importance: in all cases except F_3^-, the total negative overlap population of the four occupied π_u orbitals is comparable ($\approx$70−150%) to overlap population of the three σ_g orbitals. Thus, both the s−p mixing and π-repulsions destabilize the three-center bonding significantly. We might note that in these systems the π orbitals could also be called lone pairs, just as in X_2 diatomics one can speak of either π and π^* filled orbitals or two X lone pairs. So the π-destabilization we refer to can be equivalently called lone-pair repulsion.

Let us now check our qualitative conclusions about the factors controlling the stability of the electron-rich three-center bonding. Figure 4 plots the total overlap population together with some orbital contributions to it vs the overlap between the s and p orbitals of neighboring atoms. Clearly, the $3\sigma_g$ contribution to OP and the total σ contribution to OP, as well as the total overlap population, are all quadratically proportional to $\langle s_C|p_T\rangle$.[49] This, however, implies that also the total contribution of π symmetry (difference between the total OP and the σ contribution, not plotted here) is proportional to $\langle s_C|p_T\rangle^2$. We would expect that total π contribution to OP should rather be proportional to a π-type overlap between the p orbitals of neighboring atoms ($\langle p_C|p_T\rangle_\pi{}^2$).

The result obtained indicates that $\langle s_C|p_T\rangle$ and $\langle p_C|p_T\rangle_\pi$ have similar functional dependences for these electron-rich systems.

To probe this point, we plot in Figure 5 the $\langle s_C|p_T\rangle$, $\langle p_C|p_T\rangle_\pi$, and $\langle s_C|s_T\rangle$ integrals, grouped by anion type. We recall that the last overlap integral determines the magnitude of the destabilizing zeroth-order interaction giving rise to $1\sigma_g$ and $2\sigma_g$ orbitals; the quantitative importance of this term is discussed below.

The linear correlation between $\langle s_C|p_T\rangle$ and $\langle p_C|p_T\rangle_\pi$ is indeed very close, except for N_3^{7-} and Sn_3^{10-}. These two exceptions

(49) We note that this functional behavior is reproduced well already at the extended Hückel level of theory. The quantitative aspects are difficult to describe with the charge-independent set of STO parameters; s and especially p orbital expansion upon reduction is a crucial factor influencing Pauli repulsions.

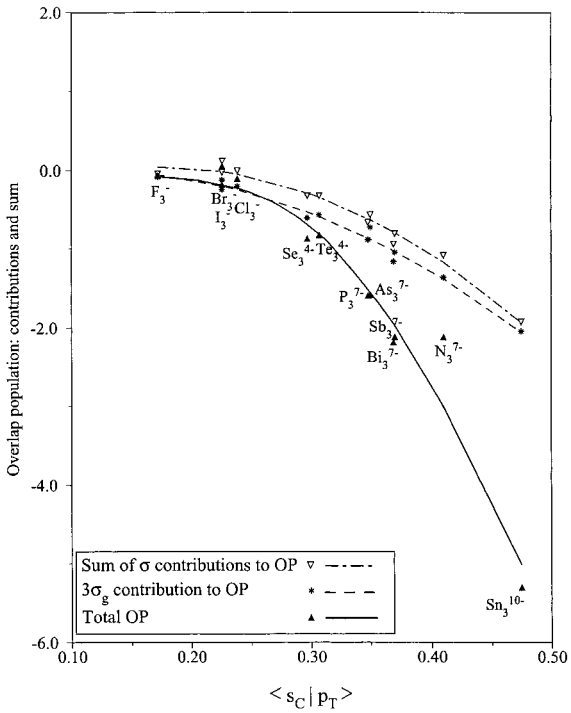

Figure 4. $3\sigma_g$ contribution to OP, sum of σ contributions to OP, and total OP vs overlap between the s and p orbitals of neighboring atoms in X_3.

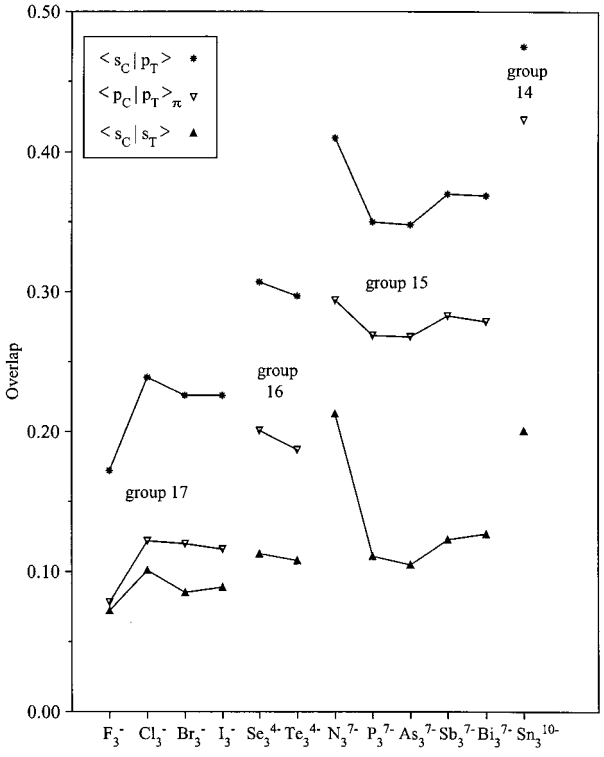

Figure 5. $\langle s_C|p_T\rangle$, $\langle p_C|p_T\rangle_\pi$, and $\langle s_C|s_T\rangle$ overlaps between central and terminal atom orbitals in X_3 as functions of the anion type.

can be traced to the relative importance of interactions between the two terminal atoms (neglected in our qualitative considerations but included in the DFT calculations). For a comparison, Figure 6 plots the $\langle p_C|p_T\rangle_\sigma$ integral, which is related to the strength of the electron-rich three-center bond between the three p_y orbitals.

Note that, in many respects, the functional behavior of the σ overlap is inverse to that of a π-type overlap between two p

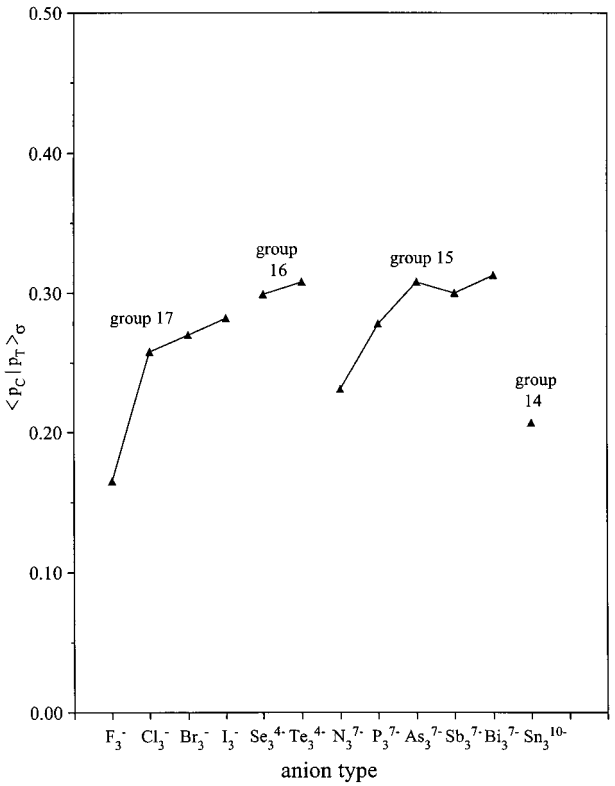

Figure 6. $\langle p_C|p_T\rangle_\sigma$ overlap between central and terminal atom orbitals in X_3 as a function of the anion type.

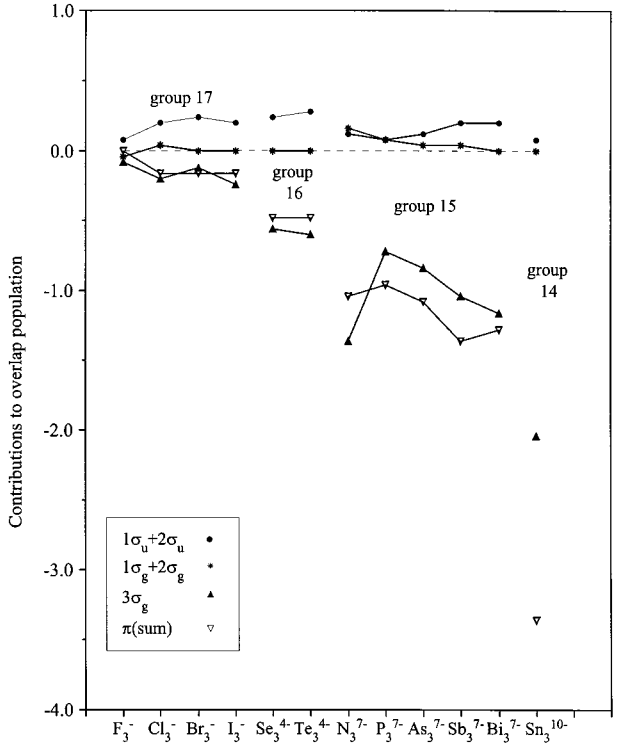

Figure 7. Orbital contributions to the overlap population as functions of the X_3 anion type.

orbitals (compare Figures 5 and 6). For example, a large decrease in the interatomic distance from P_3^{7-} to N_3^{7-} enhances the $\langle p_C|p_T\rangle_\pi$ overlap but diminishes the $\langle p_C|p_T\rangle_\sigma$ overlap. This suggests that the bond length used for our N_3^{7-} calculation is shorter than optimal for the $\langle p_C|p_T\rangle_\sigma$ overlap. In fact, this has been confirmed by our calculations for N_3^{7-} and for other electron-rich systems included in this study as well.

Let us look in more detail at the contributions to the total overlap population. The $3\sigma_g$ and $2\pi_u$ orbitals give the largest contributions to the total OP (Table 1). This is consistent with their position as frontier orbitals: They possess the highest number of nodal planes, thus the largest AO coefficients, and consequently (in absolute value) the biggest contributions to the overlap populations. The contribution of $2\pi_u$ is partly compensated by the bonding $1\pi_u$ orbitals, but this compensation is of little effect for highly charged anions. Consequently, the main feature of the π antibonding interactions is their steep increase with the charge of the system, as may be seen in Figure 7. Note the correlation between the $1\pi_u + 1\pi_g + 2\pi_u$ overlap population (Figure 7) and the $\langle p_C|p_T\rangle_\pi$ overlap (Figure 5).

It is important to point out here how far, in one important sense, we have moved from the simple Rundle−Pimentel picture: the supposedly nonbonding middle orbital of the three-center scheme (Ψ_2 in structure **1**) is actually antibonding, to a variable degree, as a result of s,p mixing.

Figures 4 and 7 illustrate the correlation between the total OP, the $3\sigma_g$ overlap population, and the type of the anion. The other two contributions of σ_g symmetry ($1\sigma_g$, $2\sigma_g$) to OP are relatively little dependent on the particular system (Table 1), and except for N_3^{7-}, they nearly completely cancel each other (Figure 7). The latter phenomenon can be understood as follows: The zeroth-order interaction between s orbitals destabilizes the antibonding ($2\sigma_g$) combination more than it stabilizes the bonding ($1\sigma_g$) one; the extent of this extra antibonding is given by the s_C,s_T orbital overlap. The first-order mixing with $3\sigma_g$ stabilizes $2\sigma_g$, due to a larger overlap and a smaller energy difference, more than $1\sigma_g$. How much larger is the overlap and how much smaller the energy difference is again determined by the s_C,s_T orbital overlap. Thus, due to s,p mixing the contribution from the lower-lying occupied orbitals to the total OP does not in fact depend on s orbital overlap and is close to zero. As a result, the highest occupied orbital dominates the total contribution of the given (σ_g) symmetry and determines the dependence of bond strength on geometrical or electronegativity perturbations. It is the Pauli principle that gives the frontier orbitals their key role in determining molecular properties.[50]

Finally, there are two occupied σ_u orbitals. The net $1\sigma_u + 2\sigma_u$ contribution is positive and (again) varies much less than the $3\sigma_g$ contribution (Figure 7). The $1\sigma_u + 2\sigma_u$ population shows some features of $\langle p_C|p_T\rangle_\sigma$ (Figure 7), but the dependence of the $1\sigma_u + 2\sigma_u$ overlap population on the system is much smaller than the $\langle p_C|p_T\rangle_\sigma$ dependence. In the absence of s,p mixing, the $1\sigma_u$ orbital would be considered as nonbonding or weakly antibonding while the $2\sigma_u$ orbital would be expected to be the main contributor to the bonding in the electron-rich three-center bond (see Figure 1). In reality, this bonding situation is found only in F_3^-, where the s−p mixing is very weak. For all other systems with a charge of −1 or −4, $1\sigma_u$ is slightly bonding. For As_3^{7-}, P_3^{7-}, N_3^{7-}, and Sn_3^{10-}, the bonding properties of $1\sigma_u$ and $2\sigma_u$ are actually switched: $1\sigma_u$ is where most of the C−T bonding is to be found, while $2\sigma_u$ becomes a nonbonding or even antibonding orbital.

(50) Hall, M. B. *Inorg. Chem.* **1978**, *17*, 2261.

Figures 4−7 not only connect the overlap population to the effective distance between the constituent atoms in the electron-rich systems but also show how the effective distance (i.e., the extent of σ and π overlapping) depends on the type of atom forming X_3, and they reveal some interesting periodic and group trends. The comparison of total overlap populations (Figure 4) and contributions to them (Figure 7) for I_3^-, Te_3^{4-}, Sb_3^{7-}, and Sn_3^{10-} shows how the stability of the system decreases with the increasing charge. What happens is a consequence of increasing $\langle s_C|p_T\rangle$ and $\langle p_C|p_T\rangle_\pi$ overlaps. The same trend is observed in the Pauli repulsion energies (not reported in detail here). A significant destabilization of Sn_3^{10-} with respect to I_3^- and Te_3^{4-} has been predicted already at the EHT level of theory.[11] The negative overlap population in Sn_3^{10-} is just so large in magnitude that this system is most unlikely to exist, no matter how well shielded by cations.

A comparison of overlap populations for electron-rich tripnictides reveals some interesting group trends. The most negative OP is found for N_3^{7-}; it increases strongly for P_3^{7-} and As_3^{7-} and again decreases for Sb_3^{7-}, Bi_3^{7-} (Figures 4 and 7). Likewise, the Pauli repulsion energies assign by far the largest destabilization to N_3^{7-} and suggest P_3^{7-} and As_3^{7-} to be more stable than Sb_3^{7-} and Bi_3^{7-}.

So, the ability to accommodate a hypervalent electron count seems to be the largest in the middle rather at the end of this group. Note also that N_3^{7-} is a unique system, not only because of the very strong destabilization of the frontier orbital but also because it is the only system where there is more contribution to the bonding from the low-lying ($1\sigma_g$, $2\sigma_g$) pair rather than from the ($1\sigma_u$, $2\sigma_u$) pair. Again the magnitude of the negative OP in N_3^{7-} makes it a poor candidate for realization.

It should be remembered that the OPs discussed throughout the paper depend on the bond lengths that are available from experiment for all group 15 ions except for N_3^{7-}. The trend of the decreasing stability for P_3^{7-}, As_3^{7-}, Sb_3^{7-}, and Bi_3^{7-} is connected to the fact that the diffuseness of the fragment s,p orbitals grows faster than the bond lengths. Our choice of the bond length in N_3^{7-} (1.75 Å) results in an OP comparable to that of Bi_3^{7-}, and one might quite naturally ask why the Bi_3^{7-} system is realized while N_3^{7-} is not. The latter fact can be rationalized in two ways. First, one should also consider the electrostatic repulsion between the fragments, which is about twice as large for N_3^{7-} as for Bi_3^{7-} and may be more difficult to compensate by the crystal field forces. Second, the crystal field and packing energies might require N_3^{7-} to adopt a shorter bond length than considered above. Our DFT calculations show that a shortening of the N−N bond length from 1.75 to 1.70 Å decreases the OP in N_3^{7-} from −2.12 to −2.46 and makes the system even more unstable.

The range of calculated overlap populations for the electron-rich trihalides is much smaller than for the group 15 hypervalent ions. F_3^- experiences much less Pauli destabilization than N_3^{7-}, and both bonding and antibonding interactions are weaker for F_3^- than for the rest of the group (Figure 7, Table 1). It is difficult (if not impossible) to predict which of the Cl_3^-, Br_3^-, I_3^- systems is most destabilized by s,p mixing. The differences in overlap populations are very small indeed, and they also depend on the bond lengths.[51] Due to a very flat energy surface, there is a large range of X−X bond lengths seen in crystal structures of the trihalides.[7] A detailed discussion of electronic structure and bonding in trihalides is given in ref 7.

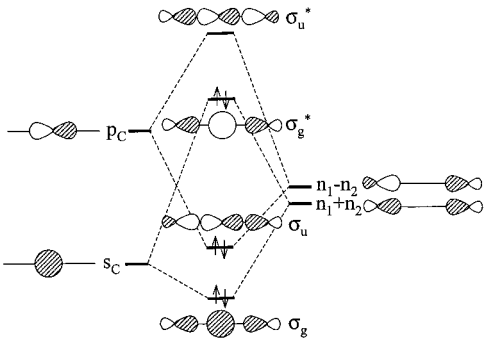

Figure 8. Simplified MO diagram summarizing the essential features of electron-rich three-center bonding, including s,p mixing, in linear X_3.

Our discussion so far focused on the orbital-interaction contributions to the chemical bonding. The electrostatic contributions are clearly important as well; for the highly negatively charged tripnictides these dominate the total bonding energy. Is the tendency of three-center systems to localize into a bond and a lone pair determined by the covalent or by the ionic driving force?

To answer this question, we have studied the effect of "hyperbolic deformation" (the replacement of a symmetrical structure, with X−X bond lengths r, by an asymmetrical one with bond lengths r_1 and r_2, where $r^2 = r_1r_2$) on the interaction energy of I_3^-, Te_3^{4-}, Sb_3^{7-}, As_3^{7-}, and P_3^{7-} when the molecule is built from three atomic fragments.[52] Our DFT calculations show that whereas the electrostatic contribution disfavors the hyperbolic stretch in all of the cases, the orbital interaction and Pauli repulsion contributions show the opposite trend. For all systems but I_3^-, the covalent (Pauli + orbital interaction) contribution decreases upon such a distortion more than the electrostatical one increases. The stretched structures are thus more stable than the symmetrical ones, and the covalent effect directs the geometrical preferences of the three-center systems. We note that the propensity of the electron-rich σ-framework in these systems to distort bears an interesting analogy to the distortive force of the electron-rich π-framework in the allyl radical and allyl anion.[53]

6. A Simpler Model and Concluding Remarks

Our detailed analysis treats the in-line bonding in X_3 as a six-orbital problem involving the top orbitals in Figure 1. Could one simplify this picture while retaining what we found to be essential in the σ system and yet different from the simplest Rundle−Pimentel picture of electron-rich three-center bonding: (1) an antibonding admixture of s_C in $3\sigma_g$ and (2) a bonding contribution of p_C in $1\sigma_u$? We think so; consider Figure 8, in which we interact s_C and p_C with two terminal atom hybrids, n_1 and n_2, forming symmetry adapted linear combinations $n_1 \pm$

(51) The dependence of the OPs on the bond lengths is, however, much weaker than for the N_3^{7-} system. For example, lengthening the bond in I_3^- from 2.93 to 3.00 Å increases the overlap population by +0.06.

(52) Structural correlations of the Bürgi−Dunitz type point to the generality of such deformations. In our case one of the bond lengths was always shortened by 0.050 Å while the other has been lengthened by 0.051 Å. The system is composed from three atomic fragments; the more distant of the terminal atoms has been assigned one electron more than the other two atoms.

(53) Shaik, S.; Shurki, A.; Danovich, D.; Hiberty, P. C. *J. Mol. Struct. (THEOCHEM)* **1997**, *155*, 398−399.

n_2[54] (we note that a similar four-orbital six-electron scheme has been previously suggested by Bigoli et al.).[55]

The actual extent of mixing will depend on the relative energies of $n_1 \pm n_2$ and s_C, p_C, as well as the relevant overlaps. Note how this picture captures the essence of important s,p mixing: σ_u is like $1\sigma_u$, σ_g* is like $3\sigma_g$. This picture also suggests that a way to think about the propensity of these systems to localize (to move to a bond and a lone pair) is to consider the localization as a second-order Jahn−Teller distortion in which σ_g* and σ_u* mix.

Here is what our perturbational analysis and the detailed density functional calculations show: The important effect of s,p mixing on the in-line bonding occurs through the destabilization of σ_g* ($3\sigma_g$) with respect to $n_1 + n_2$, which is in turn determined by the overlap between s_C and p_T. Another major contributor (destabilizing, antibonding) comes from the repulsion of p_π lone pairs, proportional to the square of the p_π–p_π overlap of the interacting atoms. Both of these antibonding effects increase with increasing negative charge of the system. Thus, the stability of isoelectronic X_3 systems decreases when moving from right to left in the periodic table.

The group trends in s,p mixing are more complex. While the overlap populations are very similar for the trihalides, they vary much more for the electron-rich tripnictides, and the ability to accommodate a hypervalent electron count seems to be the largest in the middle rather at the end of the latter group. Particularly strong s,p mixing can reverse the bonding character of MOs: For trihalides and trichalcogenides, the bonding MO is always $2\sigma_u$ and MO $1\sigma_u$ is essentially nonbonding; for tripnictides and Sn_3^{10-}, $1\sigma_u$ contributes to the bonding about as much as $1\sigma_g$, whereas $2\sigma_u$ is for P_3^{7-}, N_3^{7-}, and Sn_3^{10-} an antibonding orbital!

We believe that the combination of the qualitative MO and DFT approaches we have applied here is a very powerful analytical tool, illustrating once more the importance of simple one-electron schemes for the understanding of chemical bonding.

Acknowledgment. We thank Drs. Martin Kaupp (University of Würzburg), Dominik Munzar (Masaryk University, Brno), and John Corbett (Iowa State University) for helpful discussions and information. M.L.M. gratefully acknowledges financial support from the J. W. Fulbright Foundation. The research at Cornell was supported by the National Science Foundation through Grant CHE-99-70089.

JA010897F

(54) We have reduced a six-orbital problem to a four-orbital problem by forming four SALCs of s_Tp_T hybrids from four pure (s_T, p_T) atomic orbitals and using only the two SALCs that "point" towards the central atom.

(55) Bigoli, F.; Deplano, P.; Ienco, A.; Mealli, C.; Mersuri, M. L.; Pellinghelli, M. A.; Pintus, G.; Saba, G.; Trogu, E. F. *Inorg. Chem.* **1999**, *38*, 4626.